Higher order hierarchical H(curl) and H(div) Legendre basis functions applied in hybrid FEM-MoM

Johannesson, Peter

2011

CODEN:LUTEDX/(TEAT-7207)/1-10/(2011)

Higher order hierarchical *H*(curl) and *H*(div) Legendre basis functions applied in hybrid FEM-MoM

Peter Johannesson

Electromagnetic Theory
Department of Electrical and Information Technology
Lund University
Sweden

Peter Johannesson
Peter.Johannesson@eit.lth.se

Department of Electrical and Information Technology
Electromagnetic Theory
Lund University
P.O. Box 118
SE-221 00 Lund
Sweden

Editor: Gerhard Kristensson

Abstract

A hybrid finite element method/method of moments (FEM/MoM) technique is used to analyze the performance of higher order hierarchical Legendre basis functions. The FEM is used to model the interior part of the computational domain and the MoM is used to model the boundaries. Higher order hierarchical $H(\text{curl})$ Legendre basis functions have been applied to represent the electric field in the three dimensional FEM and higher order hierarchical $H(\text{div})$ Legendre basis functions have been applied to represent the electric and magnetic surface current densities in the MoM. The basis functions have been developed for hexahedral volume elements and quadrilateral surface elements, respectively. Numerical results are presented for the bistatic RCS of a dielectric cube for which the number of cells and the order numbers of the polynomials are varied.

1 Introduction

The hybrid FEM-MoM formulation is a powerful technique for computing the scattering fields of inhomogeneous objects. In comparison to the FEM formulation the number of degrees of freedom (DOF) is, in general, much smaller since the large surrounding space that must be inserted around the geometry in FEM in order to model the free space can be avoided. In contrast to the MoM formulation, *i.e.*, the boundary element method, the scattering properties of inhomogeneous objects can be computed. In order to solve the corresponding problem using an integral equation the volume formulation of the MoM has to be applied. This leads to six folded integrals which drastically decreases the efficiency of the method.

In the FEM-MoM formulation the scattering object is divided into an interior and exterior problem. The interior region is modeled by the FEM using higher order hierarchical $H(\text{curl})$ basis functions and the exterior region is modeled by the MoM in which higher order hierarchical $H(\text{div})$ basis functions are applied. The two formulations are then coupled by using the boundary conditions of the different fields that are included in the formulation.

It can be shown that the efficiency and accuracy of the FEM-MoM method depends highly on the formulation and discretization of the integral equation used in the MoM [2]. It is of importance to choose a proper space of test functions, especially in the case of internal resonances. Since this demand is less critical when the frequency of operation does not coincide with the frequencies of internal resonances, we have chosen to evaluate the proposed method when internal resonances do not occur.

As an example we have chosen to compute the bistatic radar cross section (RCS) of a dielectric cube, see Figure 1. In order to evaluate the proposed method, and the efficiency of the higher order basis functions, the cube has been divided into a set of equally sized hexahedral cells whereafter the p-convergence of the method has been studied.

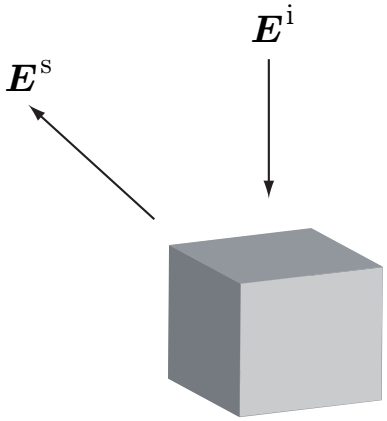

Figure 1: Geometry of the scattering object.

2 Basis functions

The basis functions that are applied in this paper are based on the $H(\mathrm{div};\Omega)$ basis functions that initially were introduced in [3]. These basis functions are defined on parameterized quadrilateral cells where each cell is spanned by the local parametric (u,v) coordinate system defined by $-1 \leq u,v \leq 1$. The $H(\mathrm{curl};\Omega)$ and $H(\mathrm{div};\Omega)$ function spaces are defined as

$$\begin{aligned} H(\mathrm{curl};\Omega) =& \{\boldsymbol{u} : \langle \boldsymbol{u},\boldsymbol{u}\rangle_\Omega < \infty,\ \langle \nabla\times\boldsymbol{u}, \nabla\times\boldsymbol{u}\rangle_\Omega < \infty\},\\ H(\mathrm{div};\Omega) =& \{\boldsymbol{u} : \langle \boldsymbol{u},\boldsymbol{u}\rangle_\Omega < \infty,\ \langle \nabla\cdot\boldsymbol{u}, \nabla\cdot\boldsymbol{u}\rangle_\Omega < \infty\}. \end{aligned}$$

The representation can be divided into three different sets: $H(\mathrm{curl};V)$, $H(\mathrm{curl};S)$ and $H(\mathrm{div};S)$ where V and S are the interior domain and the boundary of the scattering object, respectively. These are applied to represent the electric and magnetic fields, $\boldsymbol{E}$ and $\boldsymbol{H}$, and the electric and magnetic surface current densities, $\boldsymbol{J}_S$ and $\boldsymbol{M}_S$, of the scattering object.

The subspace used in the finite element (FE) implementation for the representation of the electric field is

$$U^f = \left\{\boldsymbol{a}^\ell H_\ell^{kmn} \in H(\mathrm{curl};V),\ \ell\in\{u,v,w\},\ k,m,n\in\mathbb{Z}^+\right\}$$

where the basis functions are developed to span the fields in parameterized hexahedral cells for which $-1 \leq u,v,w \leq 1$. The scalar functions are defined as

$$\begin{cases} H_u^{kmn}(u,v,w) = \widetilde{C}_k\widetilde{P}_k(v)\widetilde{C}_m\widetilde{P}_m(w)C_nP_n(u),\\ H_v^{kmn}(u,v,w) = \widetilde{C}_k\widetilde{P}_k(w)\widetilde{C}_m\widetilde{P}_m(u)C_nP_n(v),\\ H_w^{kmn}(u,v,w) = \widetilde{C}_k\widetilde{P}_k(u)\widetilde{C}_m\widetilde{P}_m(v)C_nP_n(w) \end{cases} \tag{2.1}$$

and

$$\boldsymbol{a}^u = \nabla u, \quad \boldsymbol{a}^v = \nabla v, \quad \boldsymbol{a}^w = \nabla w$$

are the contravariant unitary vectors. These are related to the covariant unitary vectors

$$\boldsymbol{a}_u = \frac{\partial \boldsymbol{r}}{\partial u}, \quad \boldsymbol{a}_v = \frac{\partial \boldsymbol{r}}{\partial v}, \quad \boldsymbol{a}_w = \frac{\partial \boldsymbol{r}}{\partial w}$$

and fulfill $\boldsymbol{a}^i \cdot \boldsymbol{a}_j = \delta_{ij}$. The functions $\widetilde{P}_m(\cdot)$ are defined as

$$\widetilde{P}_m(\cdot) = \begin{cases} 1 - (\cdot), & m = 0, \\ 1 + (\cdot), & m = 1, \\ P_m(\cdot) - P_{m-2}(\cdot), & m \geq 2, \end{cases}$$

where P_n are the Legendre polynomials and the coefficients are defined as

$$\widetilde{C}_m = \begin{cases} \frac{\sqrt{3}}{4}, & m = 0, 1, \\ \frac{1}{2}\sqrt{\frac{(2m-3)(2m+1)}{2m-1}}, & m \geq 2, \end{cases}$$
$$C_n = \sqrt{n + \frac{1}{2}}.$$

The basis functions can be divided into three classes: edge functions, surface functions and interior functions. The edge functions are represented by

$$\boldsymbol{a}^\ell H_\ell^{00n}, \quad \boldsymbol{a}^\ell H_\ell^{01n}, \quad \boldsymbol{a}^\ell H_\ell^{10n}, \quad \boldsymbol{a}^\ell H_\ell^{11n}, \quad \ell \in \{u, v, w\}, \quad n \geq 0,$$

the surface functions are represented by

$$\boldsymbol{a}^\ell H_\ell^{k0n}, \quad \boldsymbol{a}^\ell H_\ell^{k1n}, \quad \boldsymbol{a}^\ell H_\ell^{0mn}, \quad \boldsymbol{a}^\ell H_\ell^{1mn}, \quad \ell \in \{u, v, w\}, \quad k, m \geq 2, \quad n \geq 0,$$

and the interior functions are represented by

$$\boldsymbol{a}^\ell H_\ell^{kmn}, \quad \ell \in \{u, v, w\}, \quad k, m \geq 2, \quad n \geq 0.$$

In order to represent the electric and the magnetic field on the boundary of the computational domain we introduce the subspace $V^f \subset U^f$ which is defined as

$$V^f = \left\{ \boldsymbol{h} \in H(\mathrm{curl}; S) : \boldsymbol{h} = \boldsymbol{g}\big|_{\boldsymbol{r} \in S},\ \boldsymbol{g} \in U^f \right\}.$$

The FE space V^f corresponds to elements in U^f that only have support in S. This conveys that instead of hexahedral cells the elements in V^f are defined on quadrilateral cells. The FE space for the electric and magnetic surface current densities is defined as

$$W^f = \left\{ \boldsymbol{f} \in H(\mathrm{div}; S) : \boldsymbol{f} = \hat{\boldsymbol{n}} \times \boldsymbol{h},\ \boldsymbol{h} \in V^f \right\}$$

where $\hat{\boldsymbol{n}}$ is the outward directed normal unit vector. Like the functions in V^f the functions in W^f are defied to only have support on quadrilateral cells on S.

3 Formulation

The interior part, V, is modeled using the FEM. From the Maxwell's equations

$$\nabla \times \boldsymbol{E} = -\mathrm{j}\omega\mu\boldsymbol{H} = -\mathrm{j}\omega\mu_0\mu_\mathrm{c}\boldsymbol{H}, \tag{3.1}$$

$$\nabla \times \boldsymbol{H} = (\sigma + \mathrm{j}\omega\epsilon)\boldsymbol{E} = \mathrm{j}\omega\epsilon_0\epsilon_\mathrm{c}\boldsymbol{E} \tag{3.2}$$

we get the Helmholtz equation for the three dimensional problem

$$\nabla \times \frac{1}{-\mathrm{j}\omega\mu_0\mu_\mathrm{c}}\nabla \times \boldsymbol{E} - \mathrm{j}\omega\epsilon_0\epsilon_\mathrm{c}\boldsymbol{E} = \boldsymbol{0}. \tag{3.3}$$

Let

$$B(\boldsymbol{w}, \boldsymbol{E}) = \int_V \boldsymbol{w} \cdot (\nabla \times \frac{1}{-\mathrm{j}\omega\mu_0\mu_\mathrm{c}}\nabla \times \boldsymbol{E})\,\mathrm{d}V - \int_V \boldsymbol{w} \cdot \mathrm{j}\omega\epsilon_0\epsilon_\mathrm{c}\boldsymbol{E}\,\mathrm{d}V$$

be a symmetric, bilinear functional where $\boldsymbol{w} \in H(\mathrm{curl}; V)$ is a proper test function. Partial integration and applying the vector identity

$$\boldsymbol{a} \cdot (\nabla \times b) = \boldsymbol{b} \cdot (\nabla \times a) - \nabla \cdot (\boldsymbol{a} \times \boldsymbol{b})$$

leads to

$$B(\boldsymbol{w}, \boldsymbol{E}) = \int_V (\nabla \times \boldsymbol{w}) \cdot (\frac{1}{-\mathrm{j}\omega\mu_0\mu_\mathrm{c}}\nabla \times \boldsymbol{E})\,\mathrm{d}V - \int_V \boldsymbol{w} \cdot \mathrm{j}\omega\epsilon_0\epsilon_\mathrm{c}\boldsymbol{E}\,\mathrm{d}V - \int_S \hat{\boldsymbol{n}} \cdot (\boldsymbol{w} \times \frac{1}{-\mathrm{j}\omega\mu_0\mu_\mathrm{c}}\nabla \times \boldsymbol{E})\,\mathrm{d}S$$

where the divergence theorem has been applied. Using (3.1) and the boundary condition $\hat{\boldsymbol{n}} \times \boldsymbol{H} = \boldsymbol{J}_S$ yields

$$B(\boldsymbol{w}, \boldsymbol{E}) = \int_V (\nabla \times \boldsymbol{w}) \cdot (\frac{1}{-\mathrm{j}\omega\mu_0\mu_\mathrm{c}}\nabla \times \boldsymbol{E})\,\mathrm{d}V - \int_V \boldsymbol{w} \cdot \mathrm{j}\omega\epsilon_0\epsilon_\mathrm{c}\boldsymbol{E}\,\mathrm{d}V + \int_S \boldsymbol{w} \cdot \boldsymbol{J}_S\,\mathrm{d}S.$$

The weak form of (3.3) is: Find $\boldsymbol{E} \in H(\mathrm{curl}; V)$ such that

$$B(\boldsymbol{w}, \boldsymbol{E}) = 0, \quad \forall \boldsymbol{w} \in H(\mathrm{curl}; V). \tag{3.4}$$

The weak form, (3.4), can not be solved as it stands since $\boldsymbol{J}_S$ is unknown. Therefore an additional equation that relates $\boldsymbol{E}$ to $\boldsymbol{J}_S$ is needed. This can be found if the boundary condition for the total electric field on the surface, S, is applied. It states

$$\boldsymbol{E}(\boldsymbol{r}) = \boldsymbol{E}^\mathrm{i}(\boldsymbol{r}) + \boldsymbol{E}^\mathrm{s}(\boldsymbol{r}), \quad \boldsymbol{r} \in S, \tag{3.5}$$

where $\boldsymbol{E}^\mathrm{i}$ and $\boldsymbol{E}^\mathrm{s}$ are the tangential components of the incident and scattered fields, respectively. The incident field is, in this problem, represented by the plane wave

$$\boldsymbol{E}^\mathrm{i}(\boldsymbol{r}) = \boldsymbol{E}_0 \mathrm{e}^{-\mathrm{j}\boldsymbol{k}\cdot\boldsymbol{r}}.$$

The scattered field can be expressed as

$$\boldsymbol{E}^\mathrm{s} = -\mathrm{j}\omega\boldsymbol{A} - \nabla\Phi - \frac{1}{\epsilon}\nabla \times \boldsymbol{F} \tag{3.6}$$

where Φ is the electric scalar potential and $\boldsymbol{A}$ and $\boldsymbol{F}$ are the magnetic and electric vector potentials, respectively. Applying the integral representations of the quantities, *i.e.*,

$$\begin{aligned}\Phi(\boldsymbol{r}) =& \frac{1}{\epsilon}\int_S \rho_S(\boldsymbol{r}')G(\boldsymbol{r},\boldsymbol{r}')\,\mathrm{d}S',\\ \boldsymbol{A}(\boldsymbol{r}) =& \mu\int_S \boldsymbol{J}_S(\boldsymbol{r}')G(\boldsymbol{r},\boldsymbol{r}')\,\mathrm{d}S',\\ \boldsymbol{F}(\boldsymbol{r}) =& \epsilon\int_S \boldsymbol{M}_S(\boldsymbol{r}')G(\boldsymbol{r},\boldsymbol{r}')\,\mathrm{d}S',\end{aligned}$$

and inserting them into (3.6) lead to

$$\begin{aligned}\boldsymbol{E}^{\mathrm{s}}(\boldsymbol{r}) = -\mathrm{j}\omega\mu\int_S \boldsymbol{J}_S(\boldsymbol{r}')G(\boldsymbol{r},\boldsymbol{r}')\,\mathrm{d}S' - \nabla\frac{1}{\epsilon}\int_S \rho_S(\boldsymbol{r}')G(\boldsymbol{r},\boldsymbol{r}')\,\mathrm{d}S'\\ - \nabla\times\int_S \boldsymbol{M}_S(\boldsymbol{r}')G(\boldsymbol{r},\boldsymbol{r}')\,\mathrm{d}S'.\end{aligned}$$

Here ρ_{S} is the electric surface charge density, ϵ and μ the permittivity and permeability of free space and $G(\boldsymbol{r},\boldsymbol{r}') = \frac{\mathrm{e}^{-\mathrm{j}k|\boldsymbol{r}-\boldsymbol{r}'|}}{4\pi|\boldsymbol{r}-\boldsymbol{r}'|}$ the Green's function of free space. Applying the continuity equation $\rho_S = \frac{\mathrm{j}}{\omega}\nabla_S\cdot\boldsymbol{J}_{\mathrm{S}}$ yields

$$\begin{aligned}\boldsymbol{E}^{\mathrm{s}}(\boldsymbol{r}) = -\mathrm{j}\omega\mu\int_S \boldsymbol{J}_S(\boldsymbol{r}')G(\boldsymbol{r},\boldsymbol{r}')\,\mathrm{d}S' - \nabla\frac{\mathrm{j}}{\omega\epsilon}\int_S \nabla'_{\mathrm{S}}\cdot\boldsymbol{J}_S(\boldsymbol{r}')G(\boldsymbol{r},\boldsymbol{r}')\,\mathrm{d}S'\\ + \hat{\boldsymbol{n}}\times\frac{\boldsymbol{M}_S(\boldsymbol{r})}{2} + \fint_S \boldsymbol{M}_S(\boldsymbol{r}')\times\nabla G(\boldsymbol{r},\boldsymbol{r}')\,\mathrm{d}S', \quad \boldsymbol{r}\in S. \quad (3.7)\end{aligned}$$

The last integral is evaluated in a Cauchy principal value sense. Insertion of (3.7) into (3.5) gives the equation for the total electric field, the EFIE,

$$\begin{aligned}\boldsymbol{E}(\boldsymbol{r}) = \boldsymbol{E}^{\mathrm{i}}(\boldsymbol{r}) - \mathrm{j}\omega\mu\int_S \boldsymbol{J}_S(\boldsymbol{r}')G(\boldsymbol{r},\boldsymbol{r}')\,\mathrm{d}S' - \nabla\frac{\mathrm{j}}{\omega\epsilon}\int_S \nabla'_{\mathrm{S}}\cdot\boldsymbol{J}_S(\boldsymbol{r}')G(\boldsymbol{r},\boldsymbol{r}')\,\mathrm{d}S'\\ + \hat{\boldsymbol{n}}\times\frac{\boldsymbol{M}_S(\boldsymbol{r})}{2} + \fint_S \boldsymbol{M}_S(\boldsymbol{r}')\times\nabla G(\boldsymbol{r},\boldsymbol{r}')\,\mathrm{d}S', \quad \boldsymbol{r}\in S.\end{aligned}$$

Using the boundary condition $\hat{\boldsymbol{n}}\times\boldsymbol{M}_{\mathrm{S}} = \boldsymbol{E}$ leads to

$$\begin{aligned}\frac{\boldsymbol{E}(\boldsymbol{r})}{2} = \boldsymbol{E}^{\mathrm{i}}(\boldsymbol{r}) - \mathrm{j}\omega\mu\int_S \boldsymbol{J}_S(\boldsymbol{r}')G(\boldsymbol{r},\boldsymbol{r}')\,\mathrm{d}S' - \nabla\frac{\mathrm{j}}{\omega\epsilon}\int_S \nabla'_S\cdot\boldsymbol{J}_S(\boldsymbol{r}')G(\boldsymbol{r},\boldsymbol{r}')\,\mathrm{d}S'\\ + \fint_S \boldsymbol{M}_S(\boldsymbol{r}')\times\nabla G(\boldsymbol{r},\boldsymbol{r}')\,\mathrm{d}S', \quad \boldsymbol{r}\in S. \quad (3.8)\end{aligned}$$

4 Discretization

The domains V and S are divided into a set of hexahedral volume cells and quadrilateral surface cells, respectively. The basis functions $\boldsymbol{g}_j \in U^f$ are used to represent

the electric field in the hexahedral cells, $\boldsymbol{h}_j \in V^f$ to represent the electric field on the quadrilateral cells and $\boldsymbol{f}_j \in W^f$ to represent the magnetic and electric surface current densities on the quadrilateral cells. In order to relate the electric field to the electric and magnetic surface current densities on S, the representation of the electric field is expanded into two different sets $\{(E_S)_j \boldsymbol{g}_j\}$ and $\{(E_V)_j \boldsymbol{g}_j\}$. The first set consists of edge and surface functions and has support in V and S. The second set consists of edge, surface and interior functions and has only support in V and vanishes thus in S. This means that it is only the edge and surface functions in $\{(E_S)_j \boldsymbol{g}_j\}$ that couple to the electric and magnetic surface current densities on S. The expansion for the electric field in the FEM formulation yields

$$\boldsymbol{E}(\boldsymbol{r}) = \sum_j (E_V)_j \boldsymbol{g}_j(\boldsymbol{r}) + \sum_j (E_S)_j \boldsymbol{g}_j(\boldsymbol{r}), \quad \boldsymbol{r} \in V, \tag{4.1}$$

where $j = (\ell, k, m, n)$ is a multiindex. The expansion for the electric field and the electric and magnetic surface current densities in the MoM formulation reads

$$\begin{aligned} \boldsymbol{E}(\boldsymbol{r}) &= \sum_j (E_S)_j \boldsymbol{h}_j(\boldsymbol{r}), \quad \boldsymbol{r} \in S, \\ \boldsymbol{J}_S(\boldsymbol{r}) &= \sum_j (J_S)_j \boldsymbol{f}_j(\boldsymbol{r}), \quad \boldsymbol{r} \in S, \\ \boldsymbol{M}_S(\boldsymbol{r}) &= -\sum_j (E_S)_j \hat{\boldsymbol{n}} \times \boldsymbol{h}_j(\boldsymbol{r}) = -\sum_j (E_S)_j \boldsymbol{f}_j(\boldsymbol{r}), \quad \boldsymbol{r} \in S. \end{aligned} \tag{4.2}$$

Applying the FE space U^f, via the expansion (4.1), in the weak form, (3.4), leads to the matrix representation

$$\begin{pmatrix} \mathbf{A}_{VV} & \mathbf{A}_{VS} \\ \mathbf{A}_{SV} & \mathbf{A}_{SS} \end{pmatrix} \begin{pmatrix} \mathbf{E}_V \\ \mathbf{E}_S \end{pmatrix} = \begin{pmatrix} \mathbf{0} & \mathbf{0} \\ \mathbf{0} & \mathbf{B}_{SS} \end{pmatrix} \begin{pmatrix} \mathbf{0} \\ \mathbf{J}_S \end{pmatrix}. \tag{4.3}$$

The matrix elements are given by

$$\begin{aligned} [\mathbf{A}_{VV}]_{ij} &= S_{ij}, & [\mathbf{A}_{VS}]_{ij} &= S_{ij}, \\ [\mathbf{A}_{SV}]_{ij} &= S_{ij}, & [\mathbf{A}_{SS}]_{ij} &= S_{ij}, \\ [\mathbf{B}_{SS}]_{ij} &= \int_S \boldsymbol{h}_i \cdot \boldsymbol{f}_j \, \mathrm{d}S \end{aligned}$$

where

$$S_{ij} = \int_V \frac{1}{\mathrm{j}\omega\mu_0\mu_\mathrm{c}} (\nabla \times \boldsymbol{g}_i) \cdot (\nabla \times \boldsymbol{g}_j) + \mathrm{j}\omega\epsilon_0\epsilon_\mathrm{c} \boldsymbol{g}_i \cdot \boldsymbol{g}_j \, \mathrm{d}V.$$

Applying the expansions (4.2) in the EFIE, (3.8), followed by a projection on the FE space of test functions, $\boldsymbol{t}_i \in W^f$, leads to the matrix representation

$$\mathbf{C}_{SS}\mathbf{J}_S = -\mathbf{D}_{SS}\mathbf{E}_S + \mathbf{F}_S \tag{4.4}$$

where the matrix elements are given by

$$[\mathbf{C}_{SS}]_{ij} = \mathrm{j}\omega\mu \iint_S \boldsymbol{t}_i \cdot \boldsymbol{f}_j G \,\mathrm{d}S' \,\mathrm{d}S - \frac{\mathrm{j}}{\omega\epsilon} \int_S \nabla_S \cdot \boldsymbol{t}_i \int_S \nabla'_S \cdot \boldsymbol{f}_j G \,\mathrm{d}S' \,\mathrm{d}S,$$
$$[\mathbf{D}_{SS}]_{ij} = \frac{1}{2} \int_S \boldsymbol{t}_i \cdot \boldsymbol{h}_j \,\mathrm{d}S + \int_S \boldsymbol{t}_i \cdot \oint_S \boldsymbol{f}_j \times \nabla G \,\mathrm{d}S' \,\mathrm{d}S,$$
$$[\mathbf{F}_S]_i = \int_S \boldsymbol{t}_i \cdot \boldsymbol{E}^{\mathrm{i}} \,\mathrm{d}S.$$

Partial integration has been applied on the second term in $[\mathbf{C}_{SS}]$ in order to let the nabla operator operate on the test function. This operation makes the integrand of the outer integral less singular. By selecting the test functions from the space W^f the TE-formulation is obtained (short for $\hat{\boldsymbol{\tau}} \cdot \boldsymbol{E}$ where $\hat{\boldsymbol{\tau}}$ denotes a unit vector tangential to S). The TE-formulation can be used for non-closed surfaces or for closed surfaces when the frequency of operation does not coincide with the frequencies of internal resonances [4]. When the frequency of operation approaches the frequencies of internal resonances the TENENH-formulation [4] is a more preferable choice.

There are three different formulations for hybrid FEM-MoM: the outward-looking, the inward-looking and the combined formulation [2]. In this paper the outward-looking formulation has been applied. This is due to that the combined formulation in general generates an ill conditioned system matrix and that the number of unknowns of the FEM portion is larger than the number of unknowns of the MoM portion. Applying this concept, the matrix representation in (4.4) is rearranged as

$$\mathbf{J}_S = -\mathbf{C}_{SS}^{-1}\mathbf{D}_{SS}\mathbf{E}_S + \mathbf{C}_{SS}^{-1}\mathbf{F}_S. \tag{4.5}$$

Insertion in (4.3) leads to the finite dimensional representation of the problem

$$\begin{pmatrix} \mathbf{A}_{VV} & \mathbf{A}_{VS} \\ \mathbf{A}_{SV} & \mathbf{A}_{SS} + \mathbf{B}_{SS}\mathbf{C}_{SS}^{-1}\mathbf{D}_{SS} \end{pmatrix} \begin{pmatrix} \mathbf{E}_V \\ \mathbf{E}_S \end{pmatrix} = \begin{pmatrix} \mathbf{0} \\ \mathbf{B}_{SS}\mathbf{C}_{SS}^{-1}\mathbf{F}_S \end{pmatrix}.$$

5 Results

The FEM-MoM formulation presented in this paper has been applied to compute the bistatic RCS of a dielectric cube with a dielectric constant of $\epsilon_{\mathrm{r}} = 4$. The side length of the cube is $a = 0.3\lambda$ where $\lambda = 0.06\,\mathrm{m}$. The bistatic RCS is defined as

$$\frac{d\sigma}{d\Omega}(\hat{\boldsymbol{r}}, \hat{\boldsymbol{k}}_i) = \frac{|\boldsymbol{F}(\hat{\boldsymbol{r}})|}{k^2\,|\boldsymbol{E}_0|}$$

where $\hat{\boldsymbol{r}}$ is the unit field vector and $\hat{\boldsymbol{k}}_i$ is the unit wave vector of the incident field. The far-field amplitude is given by

$$\boldsymbol{F}(\hat{\boldsymbol{r}}) = \mathrm{j}\frac{k^2}{4\pi}\hat{\boldsymbol{r}} \times \int_S [\boldsymbol{M}_S(\boldsymbol{r}') + \eta_0\eta\hat{\boldsymbol{r}} \times \boldsymbol{J}_S(\boldsymbol{r}')]\mathrm{e}^{\mathrm{j}k\hat{\boldsymbol{r}}\cdot\boldsymbol{r}'} \,\mathrm{d}S'.$$

Since the surrounding medium is air, the wave vector and the wave impedance become $k = k_0$ and $\eta = 1$, respectively. The amplitude of the incident field, E_0, is set to unity, for simplicity.

In order to measure the accuracy of the method a relative error is introduced. It is defined as

$$\eta_{\mathrm{h}} = \frac{\left\| \left(\frac{d\sigma}{d\Omega}\right)_{\mathrm{h}} - \left(\widetilde{\frac{d\sigma}{d\Omega}}\right)_{\mathrm{h}} \right\|_{L^2(\Omega)}}{\left\| \left(\widetilde{\frac{d\sigma}{d\Omega}}\right)_{\mathrm{h}} \right\|_{L^2(\Omega)}}, \quad \eta_{\mathrm{v}} = \frac{\left\| \left(\frac{d\sigma}{d\Omega}\right)_{\mathrm{v}} - \left(\widetilde{\frac{d\sigma}{d\Omega}}\right)_{\mathrm{v}} \right\|_{L^2(\Omega)}}{\left\| \left(\widetilde{\frac{d\sigma}{d\Omega}}\right)_{\mathrm{v}} \right\|_{L^2(\Omega)}}.$$

The relative error has been computed in an $L^2(\Omega)$ sense where $\Omega = [0, \pi]$ is the domain of scattering angles. Index h indicates that the summation has been performed in the orthogonal direction to the $\boldsymbol{E}_0$, for which $\phi = 0$, and index v in the parallel direction, for which $\phi = \frac{\pi}{2}$, where ϕ is the azimuth angle. The reference value is represented by $\widetilde{\frac{d\sigma}{d\Omega}}$. The MoM, in the software tool FEKO, has been applied to compute the reference values. The MoM is known to produce an accurate solution but it can only be applied to homogeneous objects.

The results are presented in Figure 2. The number of unknowns for the reference

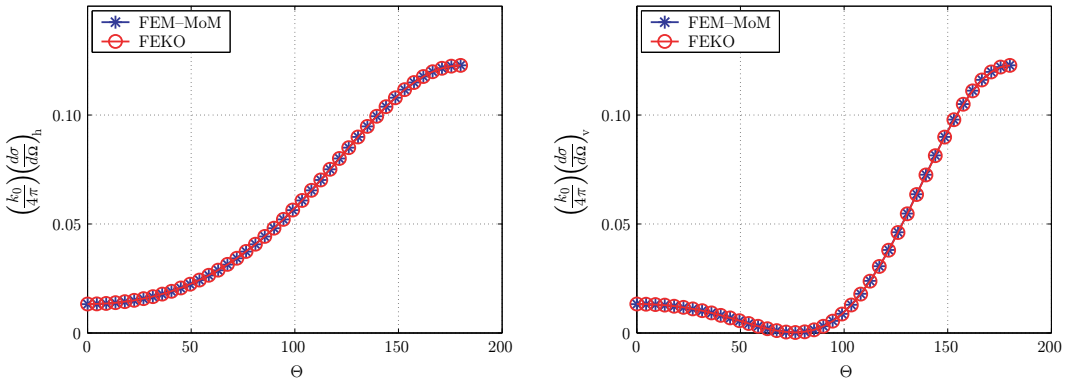

Figure 2: The bistatic RCS of a dielectric cube. The left figure corresponds to the h-polarization and the right to the v-polarization. The results from the method applied in this paper are denoted by FEM-MoM and the reference results by FEKO.

results is in the order of 10^4 and 10^3 for the FEM-MoM results. In the FEM-MoM representation, 27 hexahedral volume cells have been applied corresponding to nine quadrilateral cells on each side. As can be seen from the results the agreement between the two methods is excellent.

In order to investigate how the error of the formulation behaves, the p-convergence of the formulation has been studied for the cases $N_x = N_y = N_z = 1$, $N_x = N_y = N_z = 2$ and $N_x = N_y = N_z = 3$, respectively. The results are presented in Figure 3 and Figure 4. The reference values, that were produced by the tool FEKO, have an accuracy of four figures of merit. This states a lower bound of the accuracy.

6 Conclusions

In this paper the higher order hierarchical $H(\mathrm{curl})$ and $H(\mathrm{div})$ Legendre basis functions have been applied in a FEM-MoM formulation. To investigate the efficiency

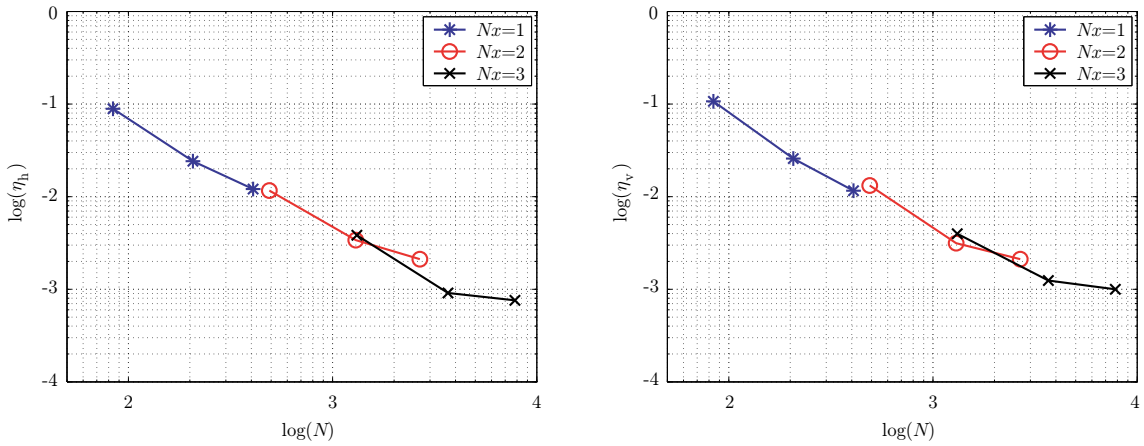

Figure 3: The relative error of the bistatic RCS of a dielectric cube as a function of the number of unknowns. The different lines correspond to different number of cells. The left figure corresponds to the h-polarization and the right to the v-polarization.

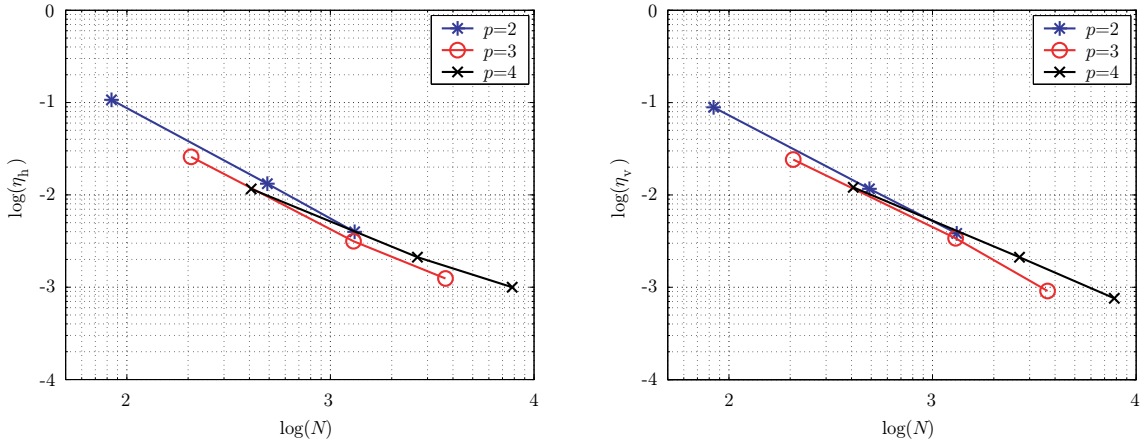

Figure 4: The relative error of the bistatic RCS of a dielectric cube as a function of the number of unknowns. The different lines correspond to different order numbers of the basis functions. The left figure corresponds to the h-polarization and the right to the v-polarization.

of the method, the bistatic RCS of a dielectric cube has been computed and the results have been compared to the MoM. The results of the FEM-MoM formulation are in excellent agreement with the results of the MoM formulation, despite that the number of unknowns of the MoM formulation is one order of magnitude greater than the number of unknowns in the FEM-MoM formulation. This is indeed remarkably, especially since the FEM-MoM formulation, in general, leads to a larger number of unknowns in comparison to the MoM. This result conveys that the memory requirements can be reduced by applying the proposed method, especially if the scattering object contains inhomogeneous medium parameters. A drawback is that it seems that the basis functions of higher order numbers are not used in an efficient way, which can be seen in Figure 4. The different lines, representing basis function of different order numbers, are overlapping which normally is not the case for p-adaptive schemes. Since the problem is not considered to include singularities, the p-dependency of the error should not be lost [1]. A possible explanation is that due to the small size of the object the field is almost constant inside the dielectric cube leading to that basis functions of higher order numbers are depressed.

References

[1] P. Ingelström. Goal-oriented adaptivity using hierarchical basis functions on tetrahedral meshes. In *Third National Conference in Computational Electromagnetics, EMB04*, October 2004.

[2] Y. Ji, H. Wang, and T. H. Hubing. A Novel Preconditioning Technique and Comparison of Three Formulations for Hybrid FEM/MoM Methods. *Appl. Computat. Electromagn. Soc. (ACES) J.*, **15**(2), 103–114, July 2000.

[3] E. Jørgensen, J. L. Volakis, P. Meincke, and O. Breinbjerg. Higher-order hierarchical Legendre basis functions for iterative integral equation solvers with curvilinear surface modeling. *Proc. IEEE Antennas Propagation Society Int. Symp.*, **4**, 618–621, June 2002.

[4] X.-Q. Sheng, J.-M. Jin, J. Song, C.-C. Lu, and W. C. Chew. On the Formulation of Hybrid Finite-Element and Boundary-Integral Methods for 3-D Scattering. *IEEE Trans. Antennas Propagat.*, **46**(3), 303–311, March 1998.